

The exclusive $\bar{B} \rightarrow \pi e^+ e^-$ and $\bar{B} \rightarrow \rho e^+ e^-$ decays in the two Higgs doublet model with flavor changing neutral currents

E. O. Iltan *

Physics Department, Middle East Technical University
Ankara, Turkey

Abstract

We calculate the leading logarithmic QCD corrections to the matrix element of the decay $b \rightarrow d e^+ e^-$ in the two Higgs doublet model with tree level flavor changing currents (model III). We continue studying the differential branching ratio and the CP violating asymmetry for the exclusive decays $B \rightarrow \pi e^+ e^-$ and $B \rightarrow \rho e^+ e^-$ and analysing the dependencies of these quantities on the selected model III parameters, $\xi^{U,D}$, including the leading logarithmic QCD corrections. Further, we present the forward-backward asymmetry of dileptons for the decay $B \rightarrow \rho e^+ e^-$ and discuss the dependencies to the model III parameters. We observe that there is a possibility to enhance the branching ratios and suppress the CP violating effects for both decays in the framework of the model III. Therefore, the measurements of these quantities will be an efficient tool to search the new physics beyond the SM.

*E-mail address: eiltan@heraklit.physics.metu.edu.tr

1 Introduction

Rare B meson decays, induced by flavor changing neutral current (FCNC) $b \rightarrow s(d)$ transitions are one of the interesting research area to test the Standard model (SM) at loop level. They are informative in the determination of the fundamental parameters, such as Cabbibo-Kobayashi-Maskawa (CKM) matrix elements, leptonic decay constants, etc. and useful for establishing the physics beyond the SM, such as two Higgs Doublet model (2HDM), Minimal Supersymmetric extension of the SM (MSSM) [1], etc.

Since the SM predicts the large Branching ratio (Br), which is measurable in the near future, the exclusive decays induced by $b \rightarrow sl^+l^-$ process become attractive. Such transitions has been investigated extensively in the SM, 2HDM and MSSM, in the literature [2]- [15]. For these transitions, the matrix element contains a term includes the virtual effects of the top quark proportional to $V_{tb}V_{ts}^*$ and additional terms describing the $c\bar{c}$ and $u\bar{u}$ loops, proportional to $V_{cb}V_{cs}^*$ and $V_{ub}V_{us}^*$ respectively. Using the unitarity of CKM matrix, i.e. $V_{ib}V_{is}^* = 0$, $i = u, c, t$, and neglecting the factor $V_{ub}V_{us}^*$ compared to $V_{tb}V_{ts}^*$ and $V_{cb}V_{cs}^*$, it is easy to see that the matrix element involves only one independent CKM factor, $V_{tb}V_{ts}^*$. This causes that the CP violating effects are suppressed within the SM [16, 17]. However, for $b \rightarrow dl^+l^-$ decay, all the CKM factors $V_{tb}V_{td}^*$, $V_{cb}V_{cd}^*$ and $V_{ub}V_{ud}^*$ are at the same order and this leads to a considerable CP violating asymmetry between the channels induced by the inclusive $b \rightarrow dl^+l^-$ and $\bar{b} \rightarrow \bar{d}l^+l^-$ decays. These effects have been studied in the literature for the inclusive $b \rightarrow de^+e^-$ decay, in the framework of the SM [18]. The difficulties of the experimental investigation of the inclusive decays stimulate the study of the exclusive decays. However, the theoretical analysis of the exclusive decays is complicated due to the hadronic form factors which can be calculated using non-perturbative methods. The dispersion formulation of the light-cone constituent quark model is one of the method which can be used to calculate the hadronic matrix elements. In the literature, the form factors for $b \rightarrow de^+e^-$ induced exclusive $B \rightarrow (\pi, \rho)e^+e^-$ decays have been calculated in the framework of this method [19, 20]. The CP violation effects for these exclusive decays have been studied in the framework of the SM [21].

In this work, we present the leading logarithmic (LLog) QCD corrected effective Hamiltonian in the 2HDM with flavor changing neutral currents (model III) for the inclusive $b \rightarrow de^+e^-$ decay and calculate the differential Br of the exclusive $\bar{B} \rightarrow (\pi, \rho)e^+e^-$ process. Further, we study the CP-violation asymmetry (A_{CP}) and forward-backward asymmetry (A_{FB}) of dileptons for the decay $\bar{B} \rightarrow \rho e^+e^-$.

The paper is organized as follows: In Section 2, we give the LLog QCD corrected Hamilto-

nian responsible for the inclusive $b \rightarrow de^+e^-$ decay and calculate the matrix element. In section 3, we present the Br and A_{CP} of the exclusive $\bar{B} \rightarrow \pi e^+e^-$ decay and analyse the dependencies of the Br and A_{CP} on the couplings $\bar{\xi}_{bb}^D, \bar{\xi}_{tt}^U$. In section 4, we study the Br, A_{CP} and A_{FB} of the exclusive $\bar{B} \rightarrow \rho e^+e^-$ decay. Section 5 is devoted to our conclusions. In Appendix, we summarize the essential points of the model III and give the explicit forms of some functions we use in our calculations.

2 Leading logarithmic improved short-distance contributions in the model III for the decay $b \rightarrow de^+e^-$ with additional long-distance effects

In this section, we present the LLog QCD corrections to the inclusive $b \rightarrow de^+e^-$ decay amplitude in the 2HDM with tree level neutral currents (model III). The LLog QCD corrections to the $b \rightarrow de^+e^-$ decay amplitude can be calculated using the effective theory. In this method, the heavy degrees of freedom, t quark, W^\pm, H^\pm, H_1 , and H_2 bosons, in the present case, are integrated out. Here H^\pm denote charged, H_1 and H_2 denote neutral Higgs bosons. The procedure is to match the full theory with the effective low energy theory at the high scale $\mu = m_W$ and evaluate the Wilson coefficients from m_W down to the lower scale $\mu \sim O(m_b)$. In our calculations we choose the higher scale as $\mu = m_W$ since the current theoretical restrictions [22, 23] show that the charged Higgs mass is enough heavy to neglect the running from m_{H^\pm} to m_W .

The effective Hamiltonian relevant for the decay $b \rightarrow de^+e^-$ in the model III is

$$\mathcal{H}_{eff} = -4 \frac{G_F}{\sqrt{2}} V_{tb} V_{td}^* \left\{ \sum_{i=1, \dots, 12} (C_i(\mu) O_i(\mu) + C'_i(\mu) O'_i(\mu)) + \lambda_u \sum_{i=1, 2, 11, 12} (C_i(\mu) (O_i(\mu) - O_i^{u'}(\mu)) + C'_i(\mu) (O'_i(\mu) - O_i^{u'}(\mu))) \right\} \quad (1)$$

where $O_i^{(\prime)}$, $O_i^{u(\prime)}$, are the operators given in eqs. (2), (3) and $C_i^{(\prime)}$ are the Wilson coefficients renormalized at the scale μ . Here the unitarity of the Kobayashi-Maskawa matrix (CKM) is used, i.e. $V_{tb} V_{td}^* + V_{ub} V_{ud}^* = -V_{cb} V_{cd}^*$ and the parameter λ_u is defined as:

$$\lambda_u = \frac{V_{ub} V_{ud}^*}{V_{tb} V_{td}^*}$$

Using Wolfenstein parametrization [24], λ_u can be written as

$$\lambda_u = \frac{\rho(1-\rho) - \eta^2}{(1-\rho)^2 + \eta^2} - i \frac{\eta}{(1-\rho)^2 + \eta^2} + O(\lambda^2)$$

where ρ , η and $\lambda \sim 0.221$ are Wolfenstein parameters. The parameter η (and therefore λ_u) is the reason for the CP violation in the SM.

The operator basis is similar to the one used for model III ([25] and references therein), which is obtained by replacing s -quark by d -quark and adding new operators, i.e. $O_i^{u(\prime)}$, $i = 1, 2, 11, 12$:

$$\begin{aligned}
O_1 &= (\bar{d}_{L\alpha}\gamma_\mu c_{L\beta})(\bar{c}_{L\beta}\gamma^\mu b_{L\alpha}), \\
O_2 &= (\bar{d}_{L\alpha}\gamma_\mu c_{L\alpha})(\bar{c}_{L\beta}\gamma^\mu b_{L\beta}), \\
O_1^u &= (\bar{d}_{L\alpha}\gamma_\mu u_{L\beta})(\bar{u}_{L\beta}\gamma^\mu b_{L\alpha}), \\
O_2^u &= (\bar{d}_{L\alpha}\gamma_\mu u_{L\alpha})(\bar{u}_{L\beta}\gamma^\mu b_{L\beta}), \\
O_3 &= (\bar{d}_{L\alpha}\gamma_\mu b_{L\alpha}) \sum_{q=u,d,s,c,b} (\bar{q}_{L\beta}\gamma^\mu q_{L\beta}), \\
O_4 &= (\bar{d}_{L\alpha}\gamma_\mu b_{L\beta}) \sum_{q=u,d,s,c,b} (\bar{q}_{L\beta}\gamma^\mu q_{L\alpha}), \\
O_5 &= (\bar{d}_{L\alpha}\gamma_\mu b_{L\alpha}) \sum_{q=u,d,s,c,b} (\bar{q}_{R\beta}\gamma^\mu q_{R\beta}), \\
O_6 &= (\bar{d}_{L\alpha}\gamma_\mu b_{L\beta}) \sum_{q=u,d,s,c,b} (\bar{q}_{R\beta}\gamma^\mu q_{R\alpha}), \\
O_7 &= \frac{e}{16\pi^2} \bar{d}_\alpha \sigma_{\mu\nu} (m_b R + m_d L) b_\alpha \mathcal{F}^{\mu\nu}, \\
O_8 &= \frac{g}{16\pi^2} \bar{d}_\alpha T_{\alpha\beta}^a \sigma_{\mu\nu} (m_b R + m_d L) b_\beta \mathcal{G}^{a\mu\nu}, \\
O_9 &= \frac{e}{16\pi^2} (\bar{d}_{L\alpha}\gamma_\mu b_{L\alpha})(\bar{l}\gamma_\mu l), \\
O_{10} &= \frac{e}{16\pi^2} (\bar{d}_{L\alpha}\gamma_\mu b_{L\alpha})(\bar{l}\gamma_\mu \gamma_5 l), \\
O_{11} &= (\bar{d}_{L\alpha}\gamma_\mu c_{L\beta})(\bar{c}_{R\beta}\gamma^\mu b_{R\alpha}), \\
O_{12} &= (\bar{d}_{L\alpha}\gamma_\mu c_{L\alpha})(\bar{c}_{R\beta}\gamma^\mu b_{R\beta}), \\
O_{11}^u &= (\bar{d}_{L\alpha}\gamma_\mu u_{L\beta})(\bar{u}_{R\beta}\gamma^\mu b_{R\alpha}), \\
O_{12}^u &= (\bar{d}_{L\alpha}\gamma_\mu u_{L\alpha})(\bar{u}_{R\beta}\gamma^\mu b_{R\beta}),
\end{aligned} \tag{2}$$

and the second operator set which are flipped chirality partners of the first:

$$\begin{aligned}
O'_1 &= (\bar{d}_{R\alpha}\gamma_\mu c_{R\beta})(\bar{c}_{R\beta}\gamma^\mu b_{R\alpha}), \\
O'_2 &= (\bar{d}_{R\alpha}\gamma_\mu c_{R\alpha})(\bar{c}_{R\beta}\gamma^\mu b_{R\beta}), \\
O_1^{\prime u} &= (\bar{d}_{R\alpha}\gamma_\mu u_{R\beta})(\bar{u}_{R\beta}\gamma^\mu b_{R\alpha}), \\
O_2^{\prime u} &= (\bar{d}_{R\alpha}\gamma_\mu u_{R\alpha})(\bar{u}_{R\beta}\gamma^\mu b_{R\beta}), \\
O'_3 &= (\bar{d}_{R\alpha}\gamma_\mu b_{R\alpha}) \sum_{q=u,d,s,c,b} (\bar{q}_{R\beta}\gamma^\mu q_{R\beta}), \\
O'_4 &= (\bar{d}_{R\alpha}\gamma_\mu b_{R\beta}) \sum_{q=u,d,s,c,b} (\bar{q}_{R\beta}\gamma^\mu q_{R\alpha}),
\end{aligned}$$

$$\begin{aligned}
O'_5 &= (\bar{d}_{R\alpha}\gamma_\mu b_{R\alpha}) \sum_{q=u,d,s,c,b} (\bar{q}_{L\beta}\gamma^\mu q_{L\beta}), \\
O'_6 &= (\bar{d}_{R\alpha}\gamma_\mu b_{R\beta}) \sum_{q=u,d,s,c,b} (\bar{q}_{L\beta}\gamma^\mu q_{L\alpha}), \\
O'_7 &= \frac{e}{16\pi^2} \bar{d}_\alpha \sigma_{\mu\nu} (m_b L + m_d R) b_\alpha \mathcal{F}^{\mu\nu}, \\
O'_8 &= \frac{g}{16\pi^2} \bar{d}_\alpha T_{\alpha\beta}^a \sigma_{\mu\nu} (m_b L + m_d R) b_\beta \mathcal{G}^{a\mu\nu}, \\
O'_9 &= \frac{e}{16\pi^2} (\bar{d}_{R\alpha}\gamma_\mu b_{R\alpha}) (\bar{l}\gamma_\mu l), \\
O'_{10} &= \frac{e}{16\pi^2} (\bar{d}_{R\alpha}\gamma_\mu b_{R\alpha}) (\bar{l}\gamma_\mu \gamma_5 l), \\
O'_{11} &= (\bar{d}_{R\alpha}\gamma_\mu c_{R\beta}) (\bar{c}_{L\beta}\gamma^\mu b_{L\alpha}), \\
O'_{12} &= (\bar{d}_{R\alpha}\gamma_\mu c_{R\alpha}) (\bar{c}_{L\beta}\gamma^\mu b_{L\beta}), \\
O'_{11}^u &= (\bar{d}_{R\alpha}\gamma_\mu u_{R\beta}) (\bar{u}_{L\beta}\gamma^\mu b_{L\alpha}), \\
O'_{12}^u &= (\bar{d}_{R\alpha}\gamma_\mu u_{R\alpha}) (\bar{u}_{L\beta}\gamma^\mu b_{L\beta}),
\end{aligned} \tag{3}$$

where α and β are $SU(3)$ colour indices and $\mathcal{F}^{\mu\nu}$ and $\mathcal{G}^{\mu\nu}$ are the field strength tensors of the electromagnetic and strong interactions, respectively.

The initial values for the first set of operators (eq.(2)) [5, 25] are

$$\begin{aligned}
C_{1,3,\dots,6,11,12}^{SM}(m_W) &= 0, \\
C_2^{SM}(m_W) &= 1, \\
C_7^{SM}(m_W) &= \frac{3x^3 - 2x^2}{4(x-1)^4} \ln x + \frac{-8x^3 - 5x^2 + 7x}{24(x-1)^3}, \\
C_8^{SM}(m_W) &= -\frac{3x^2}{4(x-1)^4} \ln x + \frac{-x^3 + 5x^2 + 2x}{8(x-1)^3}, \\
C_9^{SM}(m_W) &= -\frac{1}{\sin^2\theta_W} B(x) + \frac{1 - 4\sin^2\theta_W}{\sin^2\theta_W} C(x) - D(x) + \frac{4}{9}, \\
C_{10}^{SM}(m_W) &= \frac{1}{\sin^2\theta_W} (B(x) - C(x)), \\
C_{1,\dots,6,11,12}^H(m_W) &= 0, \\
C_7^H(m_W) &= \frac{1}{m_t^2} (\bar{\xi}_{N,tt}^U + \bar{\xi}_{N,tc}^U \frac{V_{cd}^*}{V_{td}^*}) (\bar{\xi}_{N,tt}^U + \bar{\xi}_{N,tc}^U \frac{V_{cb}}{V_{tb}}) F_1(y), \\
&+ \frac{1}{m_t m_b} (\bar{\xi}_{N,tt}^U + \bar{\xi}_{N,tc}^U \frac{V_{cd}^*}{V_{td}^*}) (\bar{\xi}_{N,bb}^D + \bar{\xi}_{N,sb}^D \frac{V_{ts}}{V_{tb}}) F_2(y), \\
C_8^H(m_W) &= \frac{1}{m_t^2} (\bar{\xi}_{N,tt}^U + \bar{\xi}_{N,tc}^U \frac{V_{cd}^*}{V_{td}^*}) (\bar{\xi}_{N,tt}^U + \bar{\xi}_{N,tc}^U \frac{V_{cb}}{V_{tb}}) G_1(y), \\
&+ \frac{1}{m_t m_b} (\bar{\xi}_{N,tt}^U + \bar{\xi}_{N,tc}^U \frac{V_{cd}^*}{V_{td}^*}) (\bar{\xi}_{N,bb}^D + \bar{\xi}_{N,sb}^D \frac{V_{ts}}{V_{tb}}) G_2(y), \\
C_9^H(m_W) &= \frac{1}{m_t^2} (\bar{\xi}_{N,tt}^U + \bar{\xi}_{N,tc}^U \frac{V_{cd}^*}{V_{td}^*}) (\bar{\xi}_{N,tt}^U + \bar{\xi}_{N,tc}^U \frac{V_{cb}}{V_{tb}}) H_1(y),
\end{aligned}$$

$$C_{10}^H(m_W) = \frac{1}{m_t^2} (\bar{\xi}_{N,tt}^U + \bar{\xi}_{N,tc}^U \frac{V_{cd}^*}{V_{td}^*}) (\bar{\xi}_{N,tt}^U + \bar{\xi}_{N,tc}^U \frac{V_{cb}}{V_{tb}}) L_1(y) , \quad (4)$$

and for the second set of operators (eq. (3)),

$$\begin{aligned} C_{1,\dots,12}^{SM}(m_W) &= 0 , \\ C_{1,\dots,6,11,12}^H(m_W) &= 0 , \\ C_7^H(m_W) &= \frac{1}{m_t^2} (\bar{\xi}_{N,bd}^D \frac{V_{tb}^*}{V_{td}^*} + \bar{\xi}_{N,sd}^D) (\bar{\xi}_{N,bb}^D + \bar{\xi}_{N,sb}^D \frac{V_{ts}}{V_{tb}}) F_1(y) , \\ &+ \frac{1}{m_t m_b} (\bar{\xi}_{N,bd}^D \frac{V_{tb}^*}{V_{td}^*} + \bar{\xi}_{N,sd}^D \frac{V_{ts}^*}{V_{td}^*}) (\bar{\xi}_{N,tt}^U + \bar{\xi}_{N,tc}^U \frac{V_{cb}}{V_{tb}}) F_2(y) , \\ C_8^H(m_W) &= \frac{1}{m_t^2} (\bar{\xi}_{N,bd}^D \frac{V_{tb}^*}{V_{td}^*} + \bar{\xi}_{N,sd}^D) (\bar{\xi}_{N,bb}^D + \bar{\xi}_{N,sb}^D \frac{V_{ts}}{V_{tb}}) G_1(y) , \\ &+ \frac{1}{m_t m_b} (\bar{\xi}_{N,bd}^D \frac{V_{tb}^*}{V_{td}^*} + \bar{\xi}_{N,sd}^D \frac{V_{ts}^*}{V_{td}^*}) (\bar{\xi}_{N,tt}^U + \bar{\xi}_{N,tc}^U \frac{V_{cb}}{V_{tb}}) G_2(y) , \\ C_9^H(m_W) &= \frac{1}{m_t^2} (\bar{\xi}_{N,bd}^D \frac{V_{tb}^*}{V_{td}^*} + \bar{\xi}_{N,sd}^D) (\bar{\xi}_{N,bb}^D + \bar{\xi}_{N,sb}^D \frac{V_{ts}}{V_{tb}}) H_1(y) , \\ C_{10}^H(m_W) &= \frac{1}{m_t^2} (\bar{\xi}_{N,bd}^D \frac{V_{tb}^*}{V_{td}^*} + \bar{\xi}_{N,sd}^D) (\bar{\xi}_{N,bb}^D + \bar{\xi}_{N,sb}^D \frac{V_{ts}}{V_{tb}}) L_1(y) , \end{aligned} \quad (5)$$

where $x = m_t^2/m_W^2$ and $y = m_t^2/m_{H^\pm}^2$. In eqs. (4) and (5) we used the redefinition

$$\xi^{U,D} = \sqrt{\frac{4G_F}{\sqrt{2}}} \bar{\xi}^{U,D} . \quad (6)$$

Here the Wilson coefficients $C_i^{SM}(m_W)$ and $C_i^H(m_W)$ denote the SM and the additional charged Higgs contributions respectively. The functions $B(x)$, $C(x)$, $D(x)$, $F_{1(2)}(y)$, $G_{1(2)}(y)$, $H_1(y)$ and $L_1(y)$ are given in appendix B. Note that in the calculations we neglect the contributions due to the neutral Higgs bosons since their interactions include negligible Yukawa couplings (see [26] for details).

Finally, the initial values of the Wilson coefficients in the model III (eqs. (4) and (5)) are

$$\begin{aligned} C_{1,3,\dots,6,11,12}^{2HDM}(m_W) &= 0 , \\ C_2^{2HDM}(m_W) &= 1 , \\ C_7^{2HDM}(m_W) &= C_7^{SM}(m_W) + C_7^H(m_W) , \\ C_8^{2HDM}(m_W) &= C_8^{SM}(m_W) + C_8^H(m_W) , \\ C_9^{2HDM}(m_W) &= C_9^{SM}(m_W) + C_9^H(m_W) , \\ C_{10}^{2HDM}(m_W) &= C_{10}^{SM}(m_W) + C_{10}^H(m_W) , \end{aligned}$$

$$C_{1,2,3,\dots,6,11,12}^{2HDM}(m_W) = 0 ,$$

$$\begin{aligned}
C_7^{\prime 2HDM}(m_W) &= C_7^{\prime SM}(m_W) + C_7^{\prime H}(m_W) , \\
C_8^{\prime 2HDM}(m_W) &= C_8^{\prime SM}(m_W) + C_8^{\prime H}(m_W) , \\
C_9^{\prime 2HDM}(m_W) &= C_9^{\prime SM}(m_W) + C_9^{\prime H}(m_W) , \\
C_{10}^{\prime 2HDM}(m_W) &= C_{10}^{\prime SM}(m_W) + C_{10}^{\prime H}(m_W) .
\end{aligned} \tag{7}$$

These initial values help us calculate the coefficients C_i^{2HDM} and $C_i^{\prime 2HDM}$ at any lower scale as in the SM ([27] references therein). The μ scale dependence of the coefficients in the LLog approximation can be found in the literature [13, 28, 29, 30]. The operators $O_5, O_6, O_{11}, O_{11}^u, O_{12}$ and O_{12}^u ($O'_5, O'_6, O'_{11}, O'_{11}^u, O'_{12}$ and O'_{12}^u) give contribution to the leading order matrix element of $b \rightarrow s\gamma$ and the magnetic moment type coefficient $C_7^{eff}(\mu)$ ($C_7^{\prime eff}(\mu)$) is redefined in the NDR scheme as:

$$\begin{aligned}
C_7^{eff}(\mu) &= C_7^{2HDM}(\mu) + Q_d (C_5^{2HDM}(\mu) + N_c C_6^{2HDM}(\mu)) , \\
&+ Q_u \left(\frac{m_c + m_u}{m_b} C_{12}^{2HDM}(\mu) + N_c \frac{m_c + m_u}{m_b} C_{11}^{2HDM}(\mu) \right) , \\
C_7^{\prime eff}(\mu) &= C_7^{\prime 2HDM}(\mu) + Q_d (C_5^{\prime 2HDM}(\mu) + N_c C_6^{\prime 2HDM}(\mu)) \\
&+ Q_u \left(\frac{m_c + m_u}{m_b} C_{12}^{\prime 2HDM}(\mu) + N_c \frac{m_c + m_u}{m_b} C_{11}^{\prime 2HDM}(\mu) \right) .
\end{aligned} \tag{8}$$

Since $O_2^{(u)}$ ($O_2^{\prime(u)}$) produce dilepton via virtual photon, their Wilson coefficient $C_2(\mu)$ ($C_2'(\mu)$) and the coefficients $C_1(\mu), C_3(\mu), \dots, C_6(\mu)$ ($C_2'(\mu), C_3'(\mu), \dots, C_6'(\mu)$) induced by the operator mixing, give contributions to $C_9^{eff}(\mu)$ ($C_9^{\prime eff}(\mu)$). In a more complete analysis, one has to take into account the long-distance (LD) contributions, produced by real $u\bar{u}, d\bar{d}$ and $c\bar{c}$ intermediate states, i.e. ρ, ω and $\psi^{(i)}, i = 1, \dots, 6$ (Table 1). These effects can be taken into account by introducing a Breit-Wigner form of the resonance propagator and it gives an additional contribution to $C_9^{eff}(\mu)$ [8, 31] ($C_9^{\prime eff}(\mu)$). Finally the effective coefficients $C_9^{eff}(\mu)$ [18, 30] and $C_9^{\prime eff}(\mu)$ are defined in the NDR scheme as:

$$\begin{aligned}
C_9^{eff}(\mu) &= C_9^{2HDM}(\mu) \tilde{\eta}(\hat{s}) + \left(h(z, \hat{s}) - \frac{3}{\alpha_{em}^2} \kappa \sum_{V_i=\psi_i} \frac{\pi \Gamma(V_i \rightarrow ll) m_{V_i}}{q^2 - m_{V_i}^2 + im_{V_i} \Gamma_{V_i}} \right) \\
&(3C_1(\mu) + C_2(\mu) + 3C_3(\mu) + C_4(\mu) + 3C_5(\mu) + C_6(\mu)) \\
&+ \lambda_u \left\{ h(z, \hat{s}) - \frac{3}{\alpha_{em}^2} \kappa \sum_{V_i=\psi_i} \frac{\pi \Gamma(V_i \rightarrow ll) m_{V_i}}{q^2 - m_{V_i}^2 + im_{V_i} \Gamma_{V_i}} \right. \\
&- \left. h(0, \hat{s}) + \frac{16\pi^2}{9} \sum_{V_j=\rho, \omega} \frac{f_{V_j}^2(q^2)/q^2}{q^2 - m_{V_j}^2 + im_{V_j} \Gamma_{V_j}} \right\} (3C_1(\mu) + C_2(\mu)) \\
&- \frac{1}{2} h(1, \hat{s}) (4C_3(\mu) + 4C_4(\mu) + 3C_5(\mu) + C_6(\mu)) \\
&- \frac{1}{2} h(0, \hat{s}) (C_3(\mu) + 3C_4(\mu)) + \frac{2}{9} (3C_3(\mu) + C_4(\mu) + 3C_5(\mu) + C_6(\mu)) ,
\end{aligned} \tag{9}$$

and

$$\begin{aligned}
C_9^{eff}(\mu) &= C_9^{2HDM}(\mu)\tilde{\eta}(\hat{s}) + \left(h(z, \hat{s}) - \frac{3}{\alpha_{em}^2}\kappa \sum_{V_i=\psi_i} \frac{\pi\Gamma(V_i \rightarrow ll)m_{V_i}}{q^2 - m_{V_i}^2 + im_{V_i}\Gamma_{V_i}} \right) \\
&\quad (3C_1'(\mu) + C_2'(\mu) + 3C_3'(\mu) + C_4'(\mu) + 3C_5'(\mu) + C_6'(\mu)) \\
&+ \lambda_u \left\{ h(z, \hat{s}) - \frac{3}{\alpha_{em}^2}\kappa \sum_{V_i=\psi_i} \frac{\pi\Gamma(V_i \rightarrow ll)m_{V_i}}{q^2 - m_{V_i}^2 + im_{V_i}\Gamma_{V_i}} \right. \\
&\quad \left. - h(0, \hat{s}) + \frac{16\pi^2}{9} \sum_{V_j=\rho, \omega} \frac{f_{V_j}^2(q^2)/q^2}{q^2 - m_{V_j}^2 + im_{V_j}\Gamma_{V_j}} \right\} (3C_1'(\mu) + C_2'(\mu)) \\
&\quad - \frac{1}{2}h(1, \hat{s}) (4C_3'(\mu) + 4C_4'(\mu) + 3C_5'(\mu) + C_6'(\mu)) \\
&\quad - \frac{1}{2}h(0, \hat{s}) (C_3'(\mu) + 3C_4'(\mu)) + \frac{2}{9} (3C_3'(\mu) + C_4'(\mu) + 3C_5'(\mu) + C_6'(\mu)) . \quad (10)
\end{aligned}$$

where $z = \frac{m_c}{m_b}$ and $\hat{s} = \frac{q^2}{m_b^2}$. In the above expression, $\tilde{\eta}(\hat{s})$ represents the one gluon correction to the matrix element O_9 with $m_d = 0$ [29] The functions $\tilde{\eta}(\hat{s})$, $\omega(\hat{s})$, $h(z, \hat{s})$ and $h(0, \hat{s})$ are given in appendix C. In eqs. (9) and (10), the phenomenological parameter $\kappa = 2.3$ is chosen to be able to reproduce the correct value of the branching ratio $Br(B \rightarrow J/\psi X \rightarrow Xl\bar{l}) = Br(B \rightarrow J/\psi X) Br(J/\psi \rightarrow Xl\bar{l})$ [10].

In the derivations of ρ and ω meson resonance effects, we used the q^2 dependence of the coupling f_{V_j} through the expression [32]

$$f_{V_j}(q^2) = f_{V_j}(0) \left(1 + \frac{q^2}{P_{V_j}(0)} (P'_{V_j}(0) + \tilde{P}_{V_j}(q^2)) \right) , \quad (11)$$

where the coupling f_{V_j} is defined as $\langle 0 | \bar{q}\gamma_\mu q | V_j(q^2) \rangle = f_{V_j}(q^2)\epsilon_\mu$, $P_{V_j}(0)$ and $P'_{V_j}(0)$ are the subtraction constants (Table (2)). The function $\tilde{P}_{V_j}(q^2)$ is [32]

$$\tilde{P}_{V_j}(q^2) = \frac{1}{16\pi^2 r} \left(-4 - \frac{20}{3}r + 4(1+2r)\left(\frac{1-r}{r}\right)^{1/2} \text{Arctan}\left(\frac{r}{1-r}\right)^{1/2} \right) , \quad (12)$$

where $r = q^2/4m_q^2$ and m_q is the mass of the quark which produces the meson. This expression is valid in the region $0 \leq q^2 \leq 4m_q^2$. For the q^2 values, $q^2 > 4m_q^2$, we use the assumption [32] $f_{V_j}(q^2) = f_{V_j}(m_{V_j}^2)$ (Table(2)).

Finally, neglecting the down quark mass, the matrix element for $b \rightarrow de^+e^-$ decay is obtained as:

$$\begin{aligned}
\mathcal{M} &= -\frac{G_F\alpha_{em}}{2\sqrt{2}\pi} V_{tb}V_{td}^* \left\{ \left(C_9^{eff}(\mu) \bar{d}\gamma_\mu(1-\gamma_5)b + C_9^{eff}(\mu) \bar{d}\gamma_\mu(1+\gamma_5)b \right) \bar{e}\gamma^\mu e \right. \\
&\quad + \left(C_{10}(\mu) \bar{d}\gamma_\mu(1-\gamma_5)b + C_{10}'(\mu) \bar{d}\gamma_\mu(1+\gamma_5)b \right) \bar{e}\gamma^\mu\gamma_5 e \\
&\quad \left. - 2 \left(C_7^{eff}(\mu) \frac{m_b}{q^2} \bar{d}i\sigma_{\mu\nu}q^\nu(1+\gamma_5)b + C_7^{eff}(\mu) \frac{m_b}{q^2} \bar{d}i\sigma_{\mu\nu}q^\nu(1-\gamma_5)b \right) \bar{e}\gamma^\mu e \right\} . \quad (13)
\end{aligned}$$

ψ	$m_\psi (GeV)$	$\Gamma(\psi \rightarrow l^+l^-) (GeV)$
J/ψ	3.097	$5.28 \cdot 10^{-6}$
$\psi^{(2)}$	3.686	$2.35 \cdot 10^{-6}$
$\psi^{(3)}$	3.770	$2.64 \cdot 10^{-7}$
$\psi^{(4)}$	4.040	$7.28 \cdot 10^{-7}$
$\psi^{(5)}$	4.160	$7.80 \cdot 10^{-7}$
$\psi^{(6)}$	4.420	$4.73 \cdot 10^{-7}$

Table 1: Masses of ψ mesons and decay widths $\Gamma(\psi \rightarrow l^+l^-)$ used in the calculations.

	$f_V(0)(GeV)$	$f_V(m_V^2)(GeV)$	$P_V(0)$	$P'_V(0)$
ρ	0.162	0.17	-0.7498	-0.0430
ω	0.166	0.180	-0.7744	-0.0430

Table 2: The decay couplings and the subtraction constants for ρ and ω mesons.

3 The exclusive $\bar{B} \rightarrow \pi e^+ e^-$ decay

3.1 The formulation

Now, we continue to present the differential decay rate and CP violating asymmetry in the process $\bar{B} \rightarrow \pi e^+ e^-$. To calculate the decay width, branching ratio, etc., for the exclusive $\bar{B} \rightarrow \pi e^+ e^-$ decay, we need the matrix elements $\langle \pi | \bar{d} \gamma_\mu (1 \pm \gamma_5) b | \bar{B} \rangle$, and $\langle \pi | \bar{d} i \sigma_{\mu\nu} q^\nu (1 \pm \gamma_5) b | \bar{B} \rangle$. Using the parametrization

$$\begin{aligned}
\langle \pi(p_\pi | \bar{d} \gamma_\mu (1 \pm \gamma_5) b | \bar{B}(p_B) \rangle &= (2p_B - q)_\mu f_+(q^2) + q_\mu f_-(q^2) , \\
\langle \pi(p_\pi | \bar{d} i \sigma_{\mu\nu} q^\nu (1 \pm \gamma_5) b | \bar{B}(p_B) \rangle &= -\{(2p_B - q)_\mu q^2 - (m_B^2 - m_\pi^2) q_\mu\} v(q^2) , \quad (14)
\end{aligned}$$

where p_B and p_π are four momentum vectors of B and π mesons respectively and $q = p_B - p_\pi$, we get the double differential decay rate:

$$\frac{d\Gamma(\bar{B} \rightarrow \pi e^+ e^-)}{d\sqrt{s} dz} = \frac{G_F^2 \alpha_{em}^2 m_B^5 |V_{tb} V_{td}^*|^2 \lambda^{1/2} \sqrt{s}}{2^{10} \pi^5} \Omega_\pi \quad (15)$$

Here

$$\Omega_\pi = \left\{ |(C_9^{eff} + C_9'^{eff}) f_+(q^2) + 2(C_7^{eff} + C_7'^{eff}) v(q^2) m_b|^2 + |(C_{10} + C_{10}') f_+(q^2)|^2 \right\} (1 - z^2) \quad (16)$$

and $z = \cos\theta$, θ is the angle between the momentum of the electron and that of B meson in the center of mass frame of the lepton pair,

$$\lambda = 1 + t^2 + s^2 - 2t - 2s - 2ts , \quad (17)$$

where $t = \frac{m_\pi^2}{m_B^2}$ and $s = \frac{q^2}{m_B^2}$.

For the form factors $f_+(q^2)$ and $v(q^2)$, we use the results due to the dispersion formulation of the light-cone constituent quark model [20]

$$\begin{aligned} f_+(q^2) &= \frac{f_+(0)}{\left(1 - \frac{q^2}{m_{f_+}^2}\right)^{2.35}}, \\ v(q^2) &= \frac{v(0)}{\left(1 - \frac{q^2}{m_v^2}\right)^{2.31}} \end{aligned} \quad (18)$$

where $f_+(0) = 0.24$, $v(0) = 0.05$ and $m_{f_+} = 6.71 \text{ GeV}$, $m_v = 6.68 \text{ GeV}$.

Let us now turn to the CP-violating asymmetry, which is defined as

$$A_{CP} = \frac{\frac{d\Gamma(\bar{B} \rightarrow \pi e^+ e^-)}{d\sqrt{s}} - \frac{d\Gamma(B \rightarrow \bar{\pi} e^+ e^-)}{d\sqrt{s}}}{\frac{d\Gamma(\bar{B} \rightarrow \pi e^+ e^-)}{d\sqrt{s}} + \frac{d\Gamma(B \rightarrow \bar{\pi} e^+ e^-)}{d\sqrt{s}}}. \quad (19)$$

The wilson coefficient C_9^{eff} is the origin of the CP violating asymmetry since it is a function of $\lambda_u = \frac{V_{ub}V_{ud}^*}{V_{tb}V_{td}^*}$. With the parametrization

$$\begin{aligned} C_9^{eff} &= \xi_1 + \lambda_u \xi_2, \\ C_9'^{eff} &= \xi_1' + \lambda_u \xi_2', \end{aligned} \quad (20)$$

and using eq. (19) we get

$$A_{CP} = -2\text{Im}(\lambda_u) \frac{\Delta_\pi}{\Omega_\pi} \lambda \quad (21)$$

where

$$\Delta_\pi = \left\{ \text{Im}(\xi_1^{t*} \xi_2^t) f_+(q^2) + 2m_b \text{Im}(\xi_2^t) (C_7^{eff} + C_7'^{eff}) \right\} v(q^2) |f_+(q^2)| \quad (22)$$

and

$$\begin{aligned} \xi_1^t &= \xi_1 + \xi_1' \\ \xi_2^t &= \xi_2 + \xi_2' \end{aligned} \quad (23)$$

In our numerical analysis we used the input values given in Table (3).

3.2 Discussion

In this section, we would like to study the q^2 dependencies of the differential Br , and A_{CP} of the decay $\bar{B} \rightarrow \pi e^+ e^-$, for the selected parameters of the model III ($\bar{\xi}_{Ntt}^U, \bar{\xi}_{Nbb}^D$), using the

Parameter	Value
m_c	1.4 (GeV)
m_b	4.8 (GeV)
α_{em}^{-1}	129
λ_t	0.04
$\Gamma_{tot}(B_d)$	$3.96 \cdot 10^{-13}$ (GeV)
m_{B_d}	5.28 (GeV)
m_ρ	0.768 (GeV)
m_π	0.139 (GeV)
m_t	175 (GeV)
m_W	80.26 (GeV)
m_Z	91.19 (GeV)
Λ_{QCD}	0.214 (GeV)
$\alpha_s(m_Z)$	0.117
$\sin\theta_W$	$\sqrt{0.2325}$

Table 3: The values of the input parameters used in the numerical calculations.

constraints [27] coming from the $\Delta F = 2$ ($F = K, D, B$) mixing ,the ρ parameter [33] and the measurement by CLEO collaboration [34],

$$Br(B \rightarrow X_s \gamma) = (2.32 \pm 0.07 \pm 0.35) 10^{-4} . \quad (24)$$

In the calculations, we take $\bar{\xi}_{Ntc} \ll \bar{\xi}_{Ntt}^U$, $\bar{\xi}_{Nbb}^D$ and $\bar{\xi}_{Nij}^D \sim 0$ where i or j are first or second generation indices (see [26] for details). Under this assumption the Wilson coefficients C'_7 , C'_9 and C'_{10} can be neglected compared to unprimed ones and the neutral Higgs contributions are suppressed.

In figs. 1 and 2 we plot the differential Br of the decay $\bar{B} \rightarrow \pi e^+ e^-$ with respect to the dilepton mass q^2 for the fixed values of $\bar{\xi}_{N,bb}^D = 40 m_b$ and charged Higgs mass $m_{H^\pm} = 400 GeV$ at the scale $\mu = m_b$. Fig. 1 represents the case where the ratio $|r_{tb}| = |\frac{\bar{\xi}_{N,tt}^U}{\bar{\xi}_{N,bb}^D}| \ll 1$. It is shown that the differential Br obtained in the model III is smaller compared to the one calculated in the SM. Fig. 2 (3) devoted to the case where $r_{tb} \gg 1$ for the fixed value of $\bar{\xi}_{N,bb}^D$, $\bar{\xi}_{N,bb}^D = 40 m_b$ ($\bar{\xi}_{N,bb}^D = 90 m_b$). The differential Br in the model III increases at this region ($r_{tb} \gg 1$) and it enhances strongly compared to the SM with the increasing $\bar{\xi}_{N,bb}^D$ (Fig. 3).

Now we present the values of Br for the $\bar{B} \rightarrow \pi e^+ e^-$ decay in the SM and model III, without LD effects. After integrating over q^2 , we get

$$Br(B \rightarrow \pi e^+ e^-) = 0.62 \times 10^{-7} \text{ (SM)} \quad (25)$$

and for the model III

$$Br(B \rightarrow K^* l^+ l^-) = \begin{cases} 0.27 \times 10^{-7} & (|r_{tb}| \ll 1, \bar{\xi}_{N,bb}^D = 40 m_b) \\ 0.54 \times 10^{-7} & (r_{tb} \gg 1, \bar{\xi}_{N,bb}^D = 40 m_b) \\ 2.65 \times 10^{-7} & (r_{tb} \gg 1, \bar{\xi}_{N,bb}^D = 90 m_b) . \end{cases} \quad (26)$$

Here, the strong enhancement of the Br can be observed for $r_{tb} \gg 1$, especially with increasing $\bar{\xi}_{N,bb}^D$. Note that, in the calculations of Br and the differential Br , we used the Wolfenstein parameters, $\rho = -0.07$, $\eta = 0.34$.

Figs. 4 and 5 show the q^2 dependence of A_{CP} for the Wolfenstein parameters $\rho = -0.07$, $\eta = 0.34$, fixed values of $\bar{\xi}_{N,bb}^D = 40 m_b$ and charged Higgs mass $m_{H^\pm} = 400 GeV$ at the scale $\mu = m_b$, for $|r_{tb}| \ll 1$ and $r_{tb} \gg 1$ respectively. The CP violation in the model III for $|r_{tb}| \ll 1$ and $\bar{\xi}_{N,bb}^D = 40 m_b$ is slightly greater than the one in the SM. However, it decreases for $r_{tb} \gg 1$ and becomes extremely smaller compared to the one calculated in the SM with increasing $\bar{\xi}_{N,bb}^D$ (Fig. 6).

We also present $\langle A_{CP} \rangle$ for two different Wolfenstein parameters in two different dilepton mass regions

(ρ, η)	SM	model III $\bar{\xi}_{bb}^D = 40 m_b$ $ r_{tb} \ll 1$	model III $\bar{\xi}_{bb}^D = 40 m_b$ $r_{tb} \gg 1$	model III $\bar{\xi}_{bb}^D = 90, m_b$ $r_{tb} \gg 1$	q^2 regions
(0.3, 0.34)	$2.20 \cdot 10^{-2}$	$2.21 \cdot 10^{-2}$	$1.58 \cdot 10^{-2}$	$0.72 \cdot 10^{-2}$	I
	$0.63 \cdot 10^{-2}$	$0.63 \cdot 10^{-2}$	$0.48 \cdot 10^{-2}$	$0.24 \cdot 10^{-2}$	II
(-0.07, 0.34)	$0.99 \cdot 10^{-2}$	$1.18 \cdot 10^{-2}$	$0.82 \cdot 10^{-2}$	$0.36 \cdot 10^{-2}$	I
	$0.32 \cdot 10^{-2}$	$0.32 \cdot 10^{-2}$	$0.24 \cdot 10^{-2}$	$0.11 \cdot 10^{-2}$	II

Table 4: The average asymmetry $\langle A_{CP} \rangle$ for regions I ($1 GeV \leq \sqrt{q^2} \leq m_{J/\psi} - 20 MeV$) and II ($m_{J/\psi} + 20 MeV \leq \sqrt{q^2} \leq m_{\psi'} - 20 MeV$)

In conclusion, we analyse the dependencies of the differential Br , Br , A_{CP} and the average CP-asymmetry $\langle A_{CP} \rangle$ on the selected model III parameters ($\bar{\xi}_{N,bb}^D, \bar{\xi}_{N,tt}^U$) for the decay $\bar{B} \rightarrow \pi e^+ e^-$. We obtain that the strong enhancement of the differential Br (Br) is possible in the framework of the model III and observe that A_{CP} is sensitive to the model III parameters ($\bar{\xi}_{N,bb}^D, \bar{\xi}_{N,tt}^U$).

4 The exclusive $\bar{B} \rightarrow \rho e^+ e^-$ decay

4.1 The formulation

In this section, we analyse the differential decay rate, A_{CP} and A_{FB} in the process $\bar{B} \rightarrow \rho e^+ e^-$. At this stage, we need the matrix elements $\langle \rho | \bar{d} \gamma_\mu (1 \pm \gamma_5) b | \bar{B} \rangle$, and $\langle \rho | \bar{d} i \sigma_{\mu\nu} q^\nu (1 \pm \gamma_5) b | \bar{B} \rangle$. Using the parametrization of the form factors as in [35], the matrix element of the $\bar{B} \rightarrow \rho e^+ e^-$ decay is obtained as [36]:

$$\begin{aligned} \mathcal{M} = & -\frac{G\alpha_{em}}{2\sqrt{2}\pi} V_{tb} V_{td}^* \left\{ \bar{\ell} \gamma^\mu \ell \left[2A_{tot} \epsilon_{\mu\nu\rho\sigma} \epsilon^{*\nu} p_\rho^\rho q^\sigma + iB_{1tot} \epsilon_\mu^* - iB_{2tot}(\epsilon^* q)(p_B + p_\rho)_\mu - iB_{3tot}(\epsilon^* q)q_\mu \right] \right. \\ & \left. + \bar{\ell} \gamma^\mu \gamma_5 \ell \left[2C_{tot} \epsilon_{\mu\nu\rho\sigma} \epsilon^{*\nu} p_\rho^\rho q^\sigma + iD_{1tot} \epsilon_\mu^* - iD_{2tot}(\epsilon^* q)(p_B + p_\rho)_\mu - iD_{3tot}(\epsilon^* q)q_\mu \right] \right\}, \quad (27) \end{aligned}$$

where $\epsilon^{*\mu}$ is the polarization vector of ρ meson, p_B and p_ρ are four momentum vectors of B and ρ mesons, $q = p_B - p_\rho$ and

$$\begin{aligned} A_{tot} &= A + A', \\ B_{1tot} &= B_1 + B'_1, \\ B_{2tot} &= B_2 + B'_2, \\ B_{3tot} &= B_3 + B'_3, \\ C_{tot} &= C + C', \\ D_{1tot} &= D_1 + D'_1, \\ D_{2tot} &= D_2 + D'_2, \\ D_{3tot} &= D_3 + D'_3. \end{aligned} \quad (28)$$

Here

$$\begin{aligned} A &= -C_9^{eff} g(q^2) + 2C_7^{eff} \frac{m_b}{q^2} g_+(q^2), \\ B_1 &= -C_9^{eff} f(q^2) + 2C_7^{eff} \frac{m_b}{q^2} \left((m_B^2 - m_\rho^2) g_+(q^2) + q^2 g_-(q^2) \right), \\ B_2 &= C_9^{eff} a_+(q^2) + 2C_7^{eff} \frac{m_b}{q^2} \left(g_+(q^2) + \frac{q^2 h(q^2)}{2} \right), \\ B_3 &= C_9^{eff} a_-(q^2) + 2C_7^{eff} \frac{m_b}{q^2} \left(g_-(q^2) - \frac{(m_B^2 - m_\rho^2) h(q^2)}{2} \right), \\ C &= -C_{10} g(q^2), \\ D_1 &= -C_{10} f(q^2), \\ D_2 &= C_{10} a_+(q^2), \end{aligned}$$

$$D_3 = C_{10} a_-(q^2), \quad (29)$$

and

$$\begin{aligned}
A' &= -C_9'^{eff} g(q^2) + 2C_7'^{eff} \frac{m_b}{q^2} g_+(q^2), \\
B_1' &= C_9'^{eff} f(q^2) - 2C_7'^{eff} \frac{m_b}{q^2} \left((m_B^2 - m_\rho^2) g_+(q^2) + q^2 g_-(q^2) \right), \\
B_2' &= -C_9'^{eff} a_+(q^2) - 2C_7'^{eff} \frac{m_b}{q^2} \left(g(q^2) + \frac{q^2 h(q^2)}{2} \right), \\
B_3' &= -C_9'^{eff} a_-(q^2) - 2C_7'^{eff} \frac{m_b}{q^2} \left(g_-(q^2) - \frac{(m_B^2 - m_\rho^2) h(q^2)}{2} \right), \\
C' &= -C_{10}' g(q^2), \\
D_1' &= C_{10}' f(q^2), \\
D_2' &= -C_{10}' a_+(q^2), \\
D_3' &= -C_{10}' a_-(q^2),
\end{aligned} \quad (30)$$

For the formfactors $g(q^2)$, $a_-(q^2)$, $a_+(q^2)$, $g_+(q^2)$, $g_-(q^2)$, $h(q^2)$, and $f(q^2)$ we use the dispersion formulation of the light-cone constituent quark model [20] in the following pole form

$$\begin{aligned}
g(q^2) &= \frac{0.036}{\left(1 - \frac{q^2}{(6.55)^2}\right)^{2.75}}, & a_+(q^2) &= \frac{-0.026}{\left(1 - \frac{q^2}{(7.29)^2}\right)^{3.04}}, \\
a_-(q^2) &= \frac{0.03}{\left(1 - \frac{q^2}{(6.88)^2}\right)^{2.85}}, & g_+(q^2) &= \frac{-0.20}{\left(1 - \frac{q^2}{(6.57)^2}\right)^{2.76}}, \\
g_-(q^2) &= \frac{0.18}{\left(1 - \frac{q^2}{(6.50)^2}\right)^{2.73}}, & h(q^2) &= \frac{0.003}{\left(1 - \frac{q^2}{(6.43)^2}\right)^{3.42}}, \\
f(q^2) &= \frac{1.10}{\left(1 - \frac{q^2}{(5.59)^2} + \left(\frac{q^2}{(7.10)^2}\right)^2\right)},
\end{aligned} \quad (31)$$

Using eq.(27), we get the double differential decay rate:

$$\begin{aligned}
\frac{d\Gamma}{dq^2 dz} &= \frac{G^2 \alpha_{em}^2 |V_{tb} V_{ts}^*|^2 \lambda^{1/2}}{2^{12} \pi^5 m_B} \left\{ 2\lambda m_B^4 \left[m_B^2 s(1+z^2) (|A_{tot}|^2 + |C_{tot}|^2) \right] \right. \\
&\quad \left. + \frac{\lambda m_B^4}{2r} \left[\lambda m_B^2 (1-z^2) (|B_{2tot}|^2 + |D_{2tot}|^2) \right] \right\}
\end{aligned}$$

$$\begin{aligned}
& + \frac{1}{2r} \left[m_B^2 \{ \lambda(1-z^2) + 8rs \} (|B_{1tot}|^2 + |D_{1tot}|^2) \right. \\
& - 2\lambda m_B^4 (1-r-s)(1-z^2) \{ Re(B_{1tot}B_{2tot}^*) + Re(D_{1tot}D_{2tot}^*) \} \left. \right] \\
& - 8m_B^4 s \lambda^{1/2} z \left[\{ Re(B_{1tot}C_{tot}^*) + Re(A_{tot}D_{1tot}^*) \} \right] \Bigg\}, \tag{32}
\end{aligned}$$

where $z = \cos\theta$, θ is the angle between the momentum of electron e and that of B meson in the center of mass frame of the lepton pair, $\lambda = 1 + t^2 + s^2 - 2t - 2s - 2ts$, $t = \frac{m_\rho^2}{m_B^2}$ and $s = \frac{q^2}{m_B^2}$.

We continue to present the CP-violating asymmetry, which is defined as in eq. (19) with the replacement of $\pi \rightarrow \rho$. Using the same parametrization as in eq. (20) we get

$$A_{CP} = -2Im(\lambda_u) \frac{\Delta_\rho}{\Omega_\rho} \lambda \tag{33}$$

where

$$\begin{aligned}
\Delta_\rho = & Im(\xi_1^{t*} \xi_2^t) \left\{ 4s m_B^2 g^2(q^2) + \frac{f^2(q^2)}{\lambda m_B^2} (6s + \frac{\lambda}{2t}) + \frac{m_B^2 \lambda}{2t} a_+^2(q^2) + \frac{(1-s-t)}{t} f(q^2) a_+(q^2) \right\} \\
& + \frac{2C_7^{eff}}{s} Im(\xi_2) \left\{ -4 \frac{(1+\sqrt{t})}{\sqrt{t}} m_b s g(q^2) g_+(q^2) - \frac{m_b}{2m_B} ((1-t)g_+(q^2) + s g_-(q^2)) (1+\sqrt{t}) \right. \\
& \left. \left(\frac{2f(q^2)}{\lambda m_B} (6s + \frac{\lambda}{2t}) + m_B a_+(q^2) \frac{1-t-s}{t} \right) + \frac{m_b}{2m_B t} \left(m_B \lambda a_+(q^2) + \frac{f(q^2)}{m_B} (1-t-s) \right) \right. \\
& \left. \left(g_+(q^2) + \frac{s m_B^2}{2} h(q^2) \right) \right\} \tag{34}
\end{aligned}$$

and

$$\begin{aligned}
\Omega_\rho = & \lambda \{ 4m_B^2 s (|A_{tot}|^2 + |C_{tot}|^2) + \frac{1}{m_B^2 \lambda} (6s + \frac{\lambda}{2t}) (|B_{1tot}|^2 + |D_{1tot}|^2) \\
& + \frac{\lambda}{2t} m_B^2 (|B_{2tot}|^2 + |D_{2tot}|^2) - \lambda \frac{1-t-s}{t} Re(B_{1tot}B_{2tot}^* + D_{1tot}D_{2tot}^*) \}. \tag{35}
\end{aligned}$$

Finally, we present A_{FB} which can give more precise information about the Wilson coefficients C_7^{eff} , C_9^{eff} and C_{10} . It is defined as:

$$A_{FB}(q^2) = \frac{\int_0^1 dz \frac{d\Gamma}{dq^2 dz} - \int_{-1}^0 dz \frac{d\Gamma}{dq^2 dz}}{\int_0^1 dz \frac{d\Gamma}{dq^2 dz} + \int_{-1}^0 dz \frac{d\Gamma}{dq^2 dz}} \tag{36}$$

After the standard calculation, we get

$$\begin{aligned}
A_{FB} = & 12 \lambda^{1/2} \frac{Re(C_{10} + C'_{10})}{\Omega_\rho} \left\{ s f(q^2) g(q^2) Re(C_9^{eff} + C_9'^{eff}) - \frac{m_b}{m_B} (C_7^{eff} + C_7'^{eff}) \right. \\
& \left. \left(m_B (1+\sqrt{t}) g(q^2) ((1-t)g_+(q^2) + s g_-(q^2)) + g_+(q^2) f(q^2) \frac{1+t}{m_B (1+\sqrt{t})} \right) \right\} \tag{37}
\end{aligned}$$

4.2 Discussion

In this section, we study the q^2 dependencies of the differential Br , A_{CP} and A_{FB} of the decay $\bar{B} \rightarrow \rho e^+ e^-$ for the selected parameters of the model III ($\bar{\xi}_{Ntt}^U$, $\bar{\xi}_{Nbb}^D$). In the calculations, we use the same restrictions for the model III parameters. (see section 3)

In figs. 7 (8) we plot the differential Br of the decay $\bar{B} \rightarrow \rho e^+ e^-$ with respect to the dilepton mass q^2 for the fixed values of $\bar{\xi}_{N,bb}^D = 40 m_b$ and charged Higgs mass $m_{H^\pm} = 400 GeV$ at the scale $\mu = m_b$, for the ratio $|r_{tb}| = \left| \frac{\bar{\xi}_{N,tt}^U}{\bar{\xi}_{N,bb}^D} \right| \ll 1$ ($r_{tb} = \frac{\bar{\xi}_{N,tt}^U}{\bar{\xi}_{N,bb}^D} \gg 1$). The differential Br , obtained in the model III, is smaller compared to the one calculated in the SM, for $|r_{tb}| \ll 1$. However, it increases at the region $r_{tb} \gg 1$ and enhances strongly compared to the SM with the increasing $\bar{\xi}_{N,bb}^D$ (Fig. 9), similar to the decay $\bar{B} \rightarrow \pi e^+ e^-$. To be complete, we present the values of Br for the $\bar{B} \rightarrow \rho e^+ e^-$ decay in the SM and model III, without the LD effects. After integrating over q^2 , we get

$$Br(\bar{B} \rightarrow \rho e^+ e^-) = 0.91 \times 10^{-7} \quad (SM) \quad (38)$$

and for the model III

$$Br(\bar{B} \rightarrow \rho e^+ e^-) = \begin{cases} 0.44 \times 10^{-7} & (|r_{tb}| \ll 1, \bar{\xi}_{N,bb}^D = 40 m_b) \\ 1.5 \times 10^{-7} & (r_{tb} \gg 1, \bar{\xi}_{N,bb}^D = 40 m_b) \\ 3.2 \times 10^{-7} & (r_{tb} \gg 1, \bar{\xi}_{N,bb}^D = 90 m_b) . \end{cases} \quad (39)$$

The strong enhancement of the Br is observed for $r_{tb} \gg 1$, especially with increasing $\bar{\xi}_{N,bb}^D$. Note that we used the Wolfenstein parameters, $\rho = -0.07$, $\eta = 0.34$, in the calculation of Br and differential Br .

Figs. 10 and 11 show the q^2 dependence of A_{CP} for the Wolfenstein parameters $\rho = -0.07$, $\eta = 0.34$, the fixed values of $\bar{\xi}_{N,bb}^D = 40 m_b$ and charged Higgs mass $m_{H^\pm} = 400 GeV$ at the scale $\mu = m_b$, for $|r_{tb}| \ll 1$ and $r_{tb} \gg 1$ respectively. The CP violation decreases in the region $r_{tb} \gg 1$, especially with increasing $\bar{\xi}_{N,bb}^D$ (Fig. 12). Now, we give $\langle A_{CP} \rangle$ for two different Wolfenstein parameters in two different dilepton mass regions

Finally, we discuss A_{FB} of the process under consideration. Figs. 13 and 14 show the q^2 dependence of A_{FB} for the Wolfenstein parameters $\rho = -0.07$, $\eta = 0.34$, the fixed values of $\bar{\xi}_{N,bb}^D = 40 m_b$ and charged Higgs mass $m_{H^\pm} = 400 GeV$ at the scale $\mu = m_b$, for $|r_{tb}| \ll 1$ and $r_{tb} \gg 1$ respectively. For $r_{tb} \gg 1$ (Fig. 13) A_{FB} changes its sign almost at $s = 0.34$, however for $r_{tb} \gg 1$ (Fig. 14) it is positive without LD effects. Therefore the determination of the sign of A_{FB} in the region $0 \leq s \leq 0.25$ (here the upper limit corresponds to the value where A_{FB} change sign in the SM) can give a unique information about the existence of the model III.

(ρ, η)	SM	model III $\xi_{bb}^D = 40m_b$ $r_{tb} \ll 1$	model III $\xi_{bb}^D = 40m_b$ $ r_{tb} > 1$	model III $\xi_{bb}^D = 90, m_b$ $ r_{tb} > 1$	q^2 regions
$(0.3, 0.34)$	$2.00 \cdot 10^{-2}$	$1.90 \cdot 10^{-2}$	$1.50 \cdot 10^{-2}$	$0.51 \cdot 10^{-2}$	I
	$0.60 \cdot 10^{-2}$	$0.57 \cdot 10^{-2}$	$0.53 \cdot 10^{-2}$	$0.25 \cdot 10^{-2}$	II
$(-0.07, 0.34)$	$0.97 \cdot 10^{-2}$	$1.00 \cdot 10^{-2}$	$0.77 \cdot 10^{-2}$	$0.34 \cdot 10^{-2}$	I
	$0.32 \cdot 10^{-2}$	$0.29 \cdot 10^{-2}$	$0.27 \cdot 10^{-2}$	$0.14 \cdot 10^{-2}$	II

Table 5: The average asymmetry $\langle A_{CP} \rangle$ for regions I ($1 \text{ GeV} \leq \sqrt{q^2} \leq m_{J/\psi} - 20 \text{ MeV}$) and II ($m_{J/\psi} + 20 \text{ MeV} \leq \sqrt{q^2} \leq m_{\psi'} - 20 \text{ MeV}$).

In conclusion, we analyse the selected model III parameters ($\bar{\xi}_{N,bb}^D, \bar{\xi}_{N,tt}^U$) dependencies of the differential Br , A_{CP} and A_{FB} of the decay $\bar{B} \rightarrow \rho e^+ e^-$. We obtain that the strong enhancement of the differential Br is possible in the framework of the model III and observe that A_{CP} and A_{FB} are very sensitive to the model III parameters ($\bar{\xi}_{N,bb}^D, \bar{\xi}_{N,tt}^U$).

5 Conclusion

We study the exclusive processes $\bar{B} \rightarrow \pi e^+ e^-$ and $\bar{B} \rightarrow \rho e^+ e^-$ which are induced by the inclusive $b \rightarrow de^+ e^-$ decay. In such type of decays, it is informative to analyse the CP violating effects, in addition to the quantities like Br , A_{FB} . The origin of the CP violation in the SM is the parameter $\lambda_u = \frac{V_{ub}V_{ud}^*}{V_{tb}V_{td}^*}$. In the model III, the couplings ξ_{ij}^U and ξ_{kl}^D ¹ can also create the CP violation in case they are not real. However, in our work disregard this possibility not to enlarge the number of free parameters and we assume that the only CP violating effect comes from the CKM matrix elements, similar to the SM.

Now, we would like to summarize the main results of our analysis:

- The Br of the exclusive decays $\bar{B} \rightarrow \pi e^+ e^-$ and $\bar{B} \rightarrow \rho e^+ e^-$ are sensitive to the model III parameters. In the region $r_{tb} \gg 1$, a strong enhancement of the Br is observed with increasing $\bar{\xi}_{bb}^D$ in both decays eqs. As an example, $Br_{noLD}(Model\ III) \sim 3Br_{noLD}(SM)$ for $\bar{\xi}_{bb}^D = 90 m_b$ (25,26) and (38,39). Therefore their experimental investigations are a crucial test for the physics beyond the SM.

- We calculated $\langle A_{CP} \rangle$ for two different invariant mass region (see Table (4) and (5)).

We observe that $\langle A_{CP} \rangle$ decreases with increasing $\bar{\xi}_{bb}^D$ for $r_{tb} \gg 1$ in both regions. For

¹Here i, j and k, l denote up and down quarks respectively.

$r_{tb} \gg 1$ and $\bar{\xi}_{bb}^D = 90 m_b$, $\langle A_{CP} \rangle$ is rather smaller compared the one in the SM, for both regions (region I and II), i.e. $\langle A_{CP} \rangle_{model III} \sim \%30 \langle A_{CP} \rangle_{SM}$.

- We calculated A_{FB} for the $\bar{B} \rightarrow \rho e^+ e^-$ decay and observe that it does not change sign in the model III if the LD effects are excluded. This shows that the determination of the sign of A_{FB} in the region $0 \leq s \leq 0.25$ will be informative to see the effects of the model III, if it exists.

As a conclusion, the experimental investigation of the quantities we present here, will be an efficient tool to search for new physics beyond the SM.

Appendix

A The essential points of the model III.

The Yukawa interaction in the general case of 2HDM (Model III) is

$$\mathcal{L}_Y = \eta_{ij}^U \bar{Q}_{iL} \tilde{\phi}_1 U_{jR} + \eta_{ij}^D \bar{Q}_{iL} \phi_1 D_{jR} + \xi_{ij}^U \bar{Q}_{iL} \tilde{\phi}_2 U_{jR} + \xi_{ij}^D \bar{Q}_{iL} \phi_2 D_{jR} + h.c. , \quad (40)$$

where L and R denote chiral projections $L(R) = 1/2(1 \mp \gamma_5)$, ϕ_i for $i = 1, 2$, are the two scalar doublets, $\eta_{ij}^{U,D}$ and $\xi_{ij}^{U,D}$ are the matrices of the Yukawa couplings. The Flavor Changing (FC) part of the interaction can be written as

$$\mathcal{L}_{Y,FC} = \xi_{ij}^U \bar{Q}_{iL} \tilde{\phi}_2 U_{jR} + \xi_{ij}^D \bar{Q}_{iL} \phi_2 D_{jR} + h.c. , \quad (41)$$

with the choice of ϕ_1 and ϕ_2

$$\phi_1 = \frac{1}{\sqrt{2}} \left[\begin{pmatrix} 0 \\ v + H^0 \end{pmatrix} + \begin{pmatrix} \sqrt{2}\chi^+ \\ i\chi^0 \end{pmatrix} \right] ; \phi_2 = \frac{1}{\sqrt{2}} \begin{pmatrix} \sqrt{2}H^+ \\ H_1 + iH_2 \end{pmatrix} . \quad (42)$$

Here the vacuum expectation values are,

$$\langle \phi_1 \rangle = \frac{1}{\sqrt{2}} \begin{pmatrix} 0 \\ v \end{pmatrix} ; \langle \phi_2 \rangle = 0 , \quad (43)$$

and the couplings $\xi^{U,D}$ for the FC charged interactions are

$$\begin{aligned} \xi_{ch}^U &= \xi_{neutral} V_{CKM} , \\ \xi_{ch}^D &= V_{CKM} \xi_{neutral} , \end{aligned} \quad (44)$$

where $\xi_{neutral}^{U,D}$ ² is defined by the expression

$$\xi_N^{U,D} = (V_L^{U,D})^{-1} \xi^{U,D} V_R^{U,D} . \quad (45)$$

Note that the charged couplings appear as a linear combinations of neutral couplings multiplied by V_{CKM} matrix elements (more details see [37]).

²In all next discussion we denote $\xi_{neutral}^{U,D}$ as $\xi_N^{U,D}$.

B The necessary functions appear in the calculation of the Wilson coefficients

The functions $B(x)$, $C(x)$, $D(x)$, $F_{1(2)}(y)$, $G_{1(2)}(y)$, $H_1(y)$ and $L_1(y)$ are given as

$$\begin{aligned}
B(x) &= \frac{1}{4} \left[\frac{-x}{x-1} + \frac{x}{(x-1)^2} \ln x \right] , \\
C(x) &= \frac{x}{4} \left[\frac{x/2-3}{x-1} + \frac{3x/2+1}{(x-1)^2} \ln x \right] , \\
D(x) &= \frac{-19x^3/36 + 25x^2/36}{(x-1)^3} + \frac{-x^4/6 + 5x^3/3 - 3x^2 + 16x/9 - 4/9}{(x-1)^4} \ln x , \\
F_1(y) &= \frac{y(7-5y-8y^2)}{72(y-1)^3} + \frac{y^2(3y-2)}{12(y-1)^4} \ln y , \\
F_2(y) &= \frac{y(5y-3)}{12(y-1)^2} + \frac{y(-3y+2)}{6(y-1)^3} \ln y , \\
G_1(y) &= \frac{y(-y^2+5y+2)}{24(y-1)^3} + \frac{-y^2}{4(y-1)^4} \ln y , \\
G_2(y) &= \frac{y(y-3)}{4(y-1)^2} + \frac{y}{2(y-1)^3} \ln y , \\
H_1(y) &= \frac{1-4\sin^2\theta_W}{\sin^2\theta_W} \frac{xy}{8} \left[\frac{1}{y-1} - \frac{1}{(y-1)^2} \ln y \right] \\
&\quad - y \left[\frac{47y^2-79y+38}{108(y-1)^3} - \frac{3y^3-6y+4}{18(y-1)^4} \ln y \right] , \\
L_1(y) &= \frac{1}{\sin^2\theta_W} \frac{xy}{8} \left[-\frac{1}{y-1} + \frac{1}{(y-1)^2} \ln y \right] .
\end{aligned} \tag{46}$$

C The functions which appear in the Wilson coefficients C_9^{eff} and $C_9'^{eff}$

The function which represents the one gluon correction to the matrix element O_9 is [29]

$$\tilde{\eta}(\hat{s}) = 1 + \frac{\alpha_s(\mu)}{\pi} \omega(\hat{s}) , \tag{47}$$

and

$$\begin{aligned}
\omega(\hat{s}) &= -\frac{2}{9}\pi^2 - \frac{4}{3}\text{Li}_2(\hat{s}) - \frac{2}{3} \ln \hat{s} \ln(1-\hat{s}) - \frac{5+4\hat{s}}{3(1+2\hat{s})} \ln(1-\hat{s}) - \\
&\quad \frac{2\hat{s}(1+\hat{s})(1-2\hat{s})}{3(1-\hat{s})^2(1+2\hat{s})} \ln \hat{s} + \frac{5+9\hat{s}-6\hat{s}^2}{6(1-\hat{s})(1+2\hat{s})} ,
\end{aligned} \tag{48}$$

$h(z, \hat{s})$ arises from the one loop contributions of the four quark operators O_1, \dots, O_6 (O'_1, \dots, O'_6)

$$h(z, \hat{s}) = -\frac{8}{9} \ln \frac{m_b}{\mu} - \frac{8}{9} \ln z + \frac{8}{27} + \frac{4}{9}x \quad (49)$$

$$-\frac{2}{9}(2+x)|1-x|^{1/2} \begin{cases} \left(\ln \left| \frac{\sqrt{1-x}+1}{\sqrt{1-x}-1} \right| - i\pi \right), & \text{for } x \equiv \frac{4z^2}{\hat{s}} < 1 \\ 2 \arctan \frac{1}{\sqrt{x-1}}, & \text{for } x \equiv \frac{4z^2}{\hat{s}} > 1, \end{cases}$$

$$h(0, \hat{s}) = \frac{8}{27} - \frac{8}{9} \ln \frac{m_b}{\mu} - \frac{4}{9} \ln \hat{s} + \frac{4}{9}i\pi, \quad (50)$$

where $z = \frac{m_c}{m_b}$ and $\hat{s} = \frac{q^2}{m_b^2}$.

References

- [1] J. L. Hewett, in proc. of the 21st Annual SLAC Summer Institute, ed. L. De Porcel and C. Dunwoode, SLAC-PUB6521.
- [2] W. S. Hou, R. S. Willey and A. Soni, *Phys. Rev. Lett.* **58** (1987) 1608.
- [3] N. G. Deshpande and J. Trampetic, *Phys. Rev. Lett.* **60** (1988) 2583.
- [4] C. S. Lim, T. Morozumi and A. I. Sanda, *Phys. Lett.* **B218** (1989) 343.
- [5] B. Grinstein, M. J. Savage and M. B. Wise, *Nucl. Phys.* **B319** (1989) 271.
- [6] C. Dominguez, N. Paver and Riazuddin, *Phys. Lett.* **B214** (1988) 459.
- [7] N. G. Deshpande, J. Trampetic and K. Ponose, *Phys. Rev.* **D39** (1989) 1461.
- [8] P. J. O'Donnell and H. K. Tung, *Phys. Rev.* **D43** (1991) 2067.
- [9] N. Paver and Riazuddin, *Phys. Rev.* **D45** (1992) 978.
- [10] A. Ali, T. Mannel and T. Morozumi, *Phys. Lett.* **B273** (1991) 505.
- [11] A. Ali, G. F. Giudice and T. Mannel, *Z. Phys.* **C67** (1995) 417.
- [12] C. Greub, A. Ioannissian and D. Wyler, *Phys. Lett.* **B346** (1995) 145;
D. Liu *Phys. Lett.* **B346** (1995) 355;
G. Burdman, *Phys. Rev.* **D52** (1995) 6400;
Y. Okada, Y. Shimizu and M. Tanaka [hep-ph/9704223](#).
- [13] A. J. Buras and M. Münz, *Phys. Rev.* **D52** (1995) 186.
- [14] N. G. Deshpande, X. -G. He and J. Trampetic, *Phys. Lett.* **B367** (1996) 362.
- [15] W. Jaus and D. Wyler, *Phys. Rev.* **D41** (1990) 3405.
- [16] T. M. Aliev, D. A. Demir, E. Iltan and N. K. Pak, *Phys. Rev.* **D54** (1996) 851.
- [17] D. S. Du and M. Z. Yang, *Phys. Rev.* **D54** (1996) 882.
- [18] F. Krüger and L. M. Sehgal *Phys. Rev.* **D55** (1997) 2799.
- [19] D. Melikhov, *Phys. Rev.* **D53** (1996) 2460.

- [20] D. Melikhov, **hep-ph/9609503**
- [21] F. Krüger and L. M. Sehgal *Phys. Rev.* **D56** (1997) 5452.
- [22] T. M. Aliev, G. Hiller and E. Iltan, *Nucl. Phys.* **B515** (1998) 321.
- [23] M. Ciuchini et al. **hep-ph/9710335**
- [24] L. Wolfenstein, *Phys. Rev. Lett.* **51** (1983) 1945.
- [25] T. M. Aliev and E. Iltan, **hep-ph/9804458**, (1998).
- [26] T. M. Aliev, and E. Iltan, **hep-ph/9803459**, (1998).
- [27] T. M. Aliev, and E. Iltan, **hep-ph/9803272**, (1998).
- [28] B. Grinstein, R. Springer, and M. Wise, *Nuc. Phys.* **B339** (1990) 269; R. Grigjanis, P.J. O'Donnell, M. Sutherland and H. Navelet, *Phys. Lett.* **B213** (1988) 355; *Phys. Lett.* **B286** (1992) E, 413; G. Cella, G. Curci, G. Ricciardi and A. Viceré, *Phys. Lett.* **B325** (1994) 227, *Nucl. Phys.* **B431** (1994) 417.
- [29] M. Misiak, *Nucl. Phys.* **B393** (1993) 23, Erratum **B439** (1995) 461.
- [30] C. Greub, A. Ioannissian, D Weyler, *Phys. Lett.* **B218** (1989) 343.
- [31] A. I. Vainshtein, V. I. Zakharov, L. B. Okun and M. A. Shifman, *Sov. J. Nucl. Phys.* **24** (1976) 427.
- [32] K. Terasaki *Nuovo Cimento* **66** (1981) 475.
- [33] D. Atwood, L. Reina and A. Soni, *Phys. Rev.* **D55** (1997) 3156.
- [34] M. S. Alam *et. al.* **CLEO** Collaboration, *Phys. Rev.Lett.* **74** (1995) 2885.
- [35] P. Colangelo, F. De Fazio, P. Santorelli and E. Scrimieri, *Phys. Rev.* **D53** (1996) 3672.
- [36] T. M. Aliev, M. Savci, A. Ozpineci and H. Koru, *Phys. Lett.* **B410** (1997) 216.
- [37] D. Atwood, L. Reina and A. Soni, *Phys. Rev.* **D53** (1996) 119.

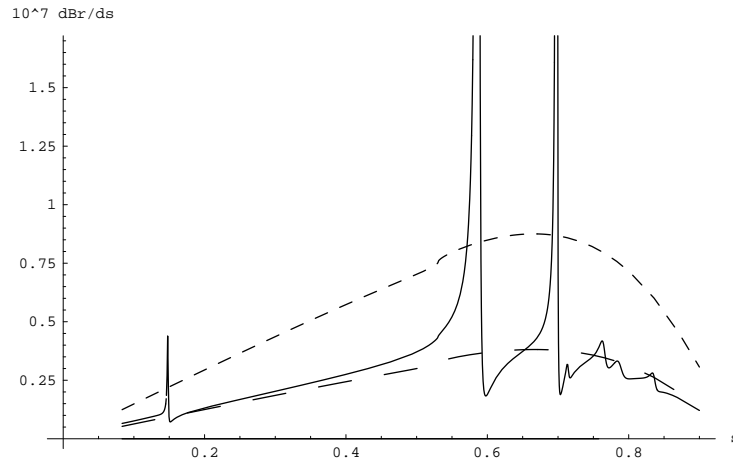


Figure 1: Differential Br as a function of q^2 for fixed $\bar{\xi}_{N,bb}^D = 40 m_b$ in the region $|r_{tb}| \ll 1$, at the scale $\mu = m_b$ for the process $\bar{B} \rightarrow \pi e^+ e^-$. Here solid line and corresponds to the model III with LD effects, dashed line to the model III without LD effects and dotted dashed line to the SM without LD effects.

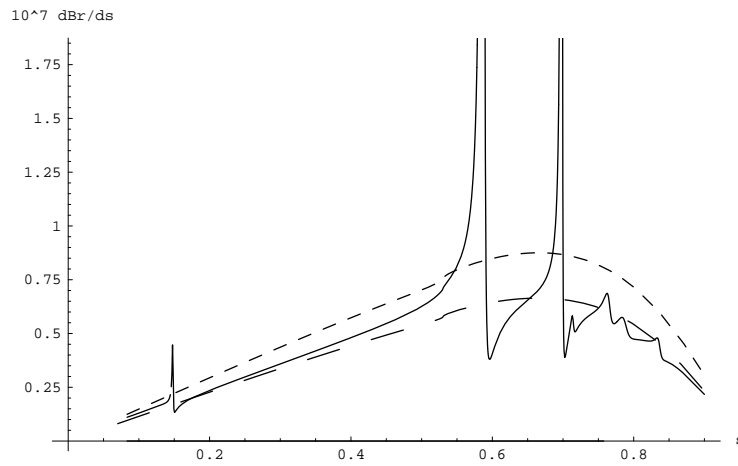


Figure 2: The same as Fig 1, but at the region $r_{tb} \gg 1$.

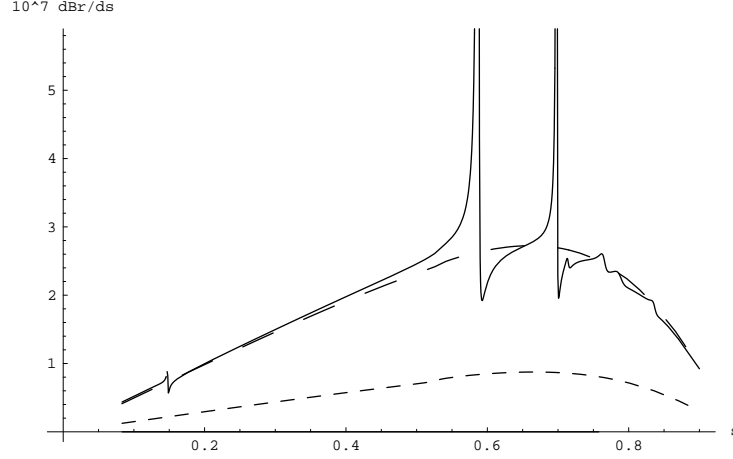


Figure 3: The same as Fig 2, but for fixed $\bar{\xi}_{N,bb}^D = 90 m_b$ value.

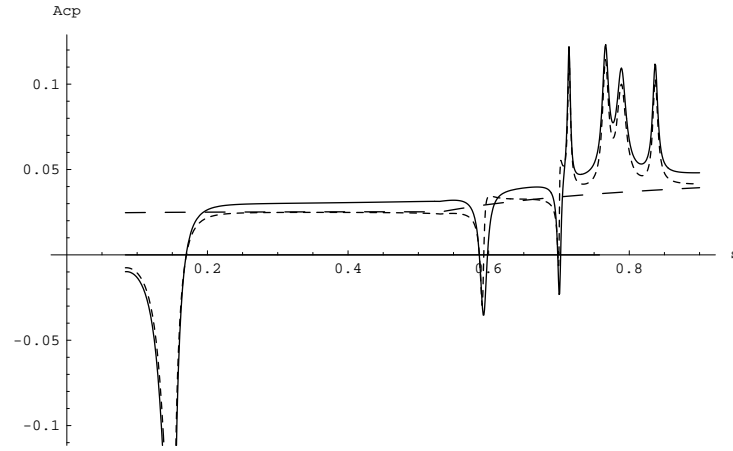


Figure 4: A_{CP} as a function of q^2 for fixed $\bar{\xi}_{N,bb}^D = 40 m_b$ in the region $|r_{tb}| \ll 1$, at the scale $\mu = m_b$, for the process $\bar{B} \rightarrow \pi e^+ e^-$. Here solid line corresponds to the model III with LD effects, dashed line to the SM without LD effects and dotted dashed line to the SM with LD effects.

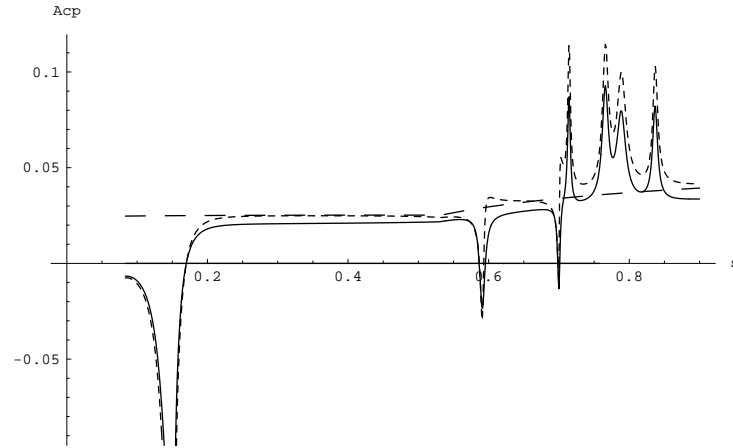


Figure 5: The same as Fig. 4, but at the region $r_{tb} \gg 1$.

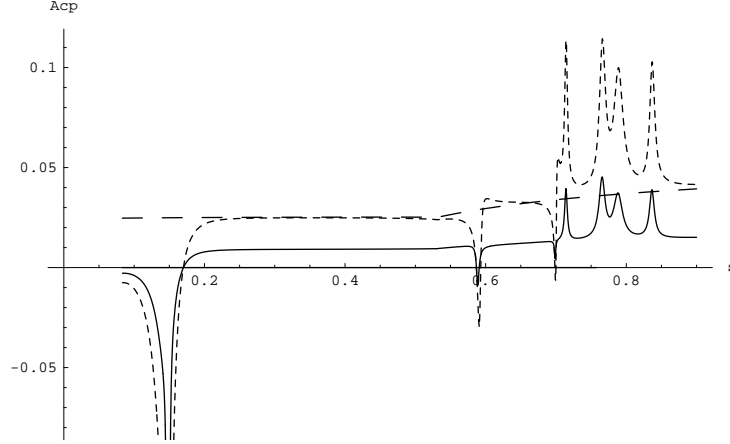


Figure 6: The same as Fig 5, but for fixed $\bar{\xi}_{N,bb}^D = 90 m_b$ value. .

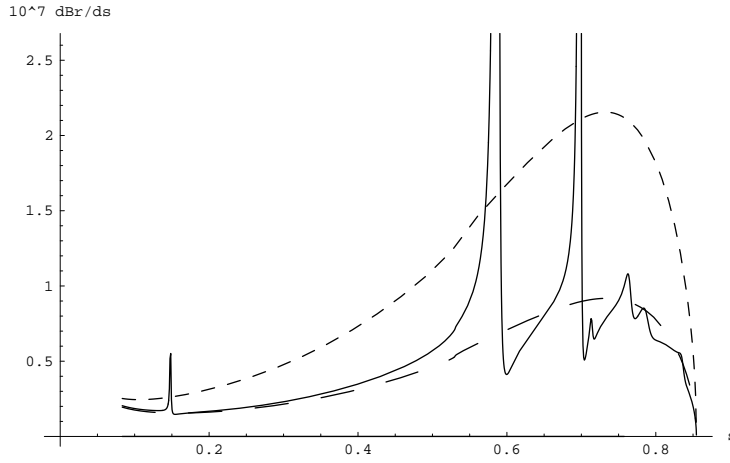


Figure 7: Differential Br as a function of q^2 for fixed $\bar{\xi}_{N,bb}^D = 40 m_b$ in the region $|r_{tb}| \ll 1$, at the scale $\mu = m_b$ for the process $\bar{B} \rightarrow \rho e^+ e^-$. Here solid line and corresponds to the model III with LD effects, dashed line to the model III without LD effects and dotted dashed line to the SM without LD effects.

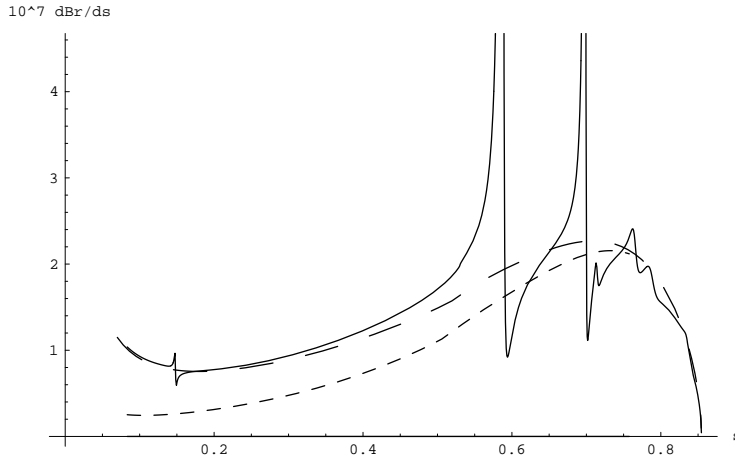


Figure 8: The same as Fig. 7, but at the region $r_{tb} \gg 1$.

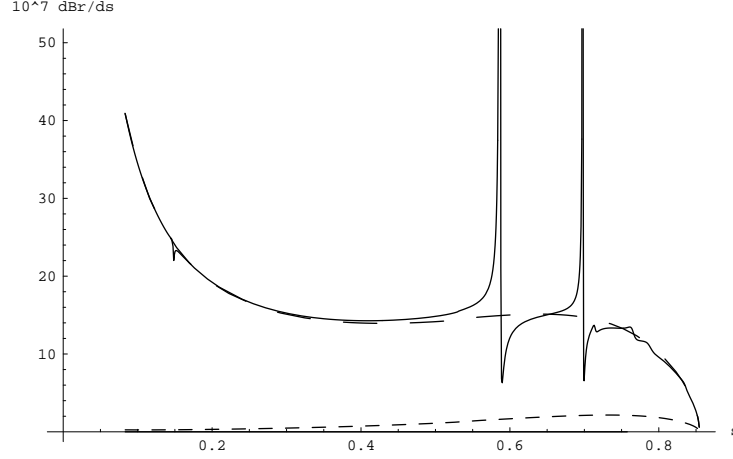


Figure 9: The same as Fig. 8, but for fixed $\bar{\xi}_{N,bb}^D = 90 m_b$ value.

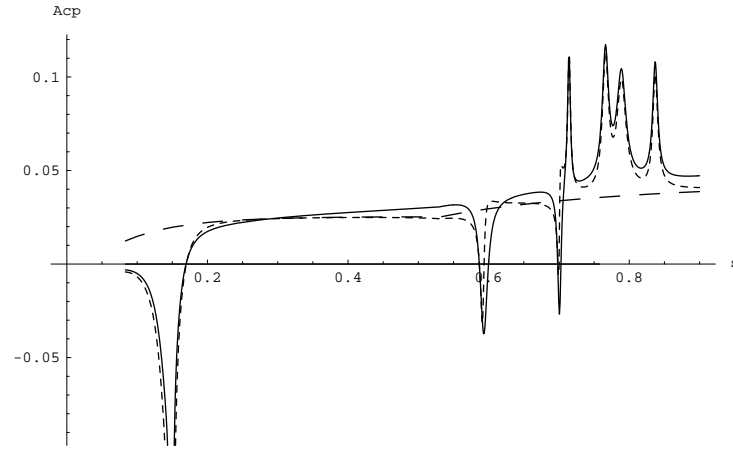


Figure 10: A_{CP} as a function of q^2 for fixed $\bar{\xi}_{N,bb}^D = 40 m_b$ in the region $|r_{tb}| \ll 1$, at the scale $\mu = m_b$, for the process $\bar{B} \rightarrow \rho e^+ e^-$. Here solid line corresponds to the model III with LD effects, dashed line to the SM without LD effects and dotted dashed line to the SM with LD effects.

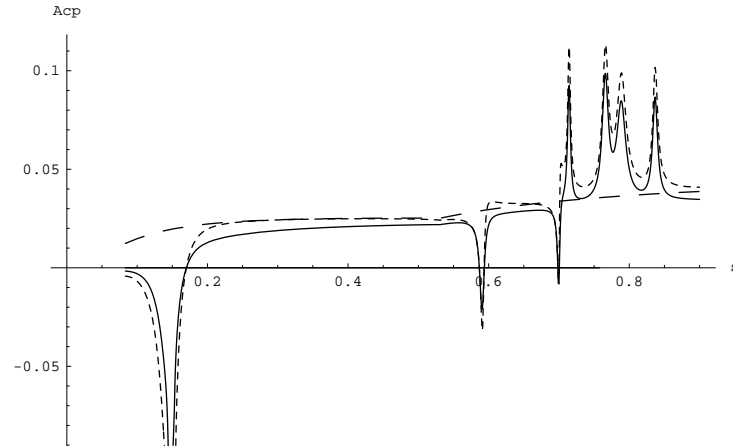


Figure 11: The same as Fig 10, but at the region $r_{tb} \gg 1$.

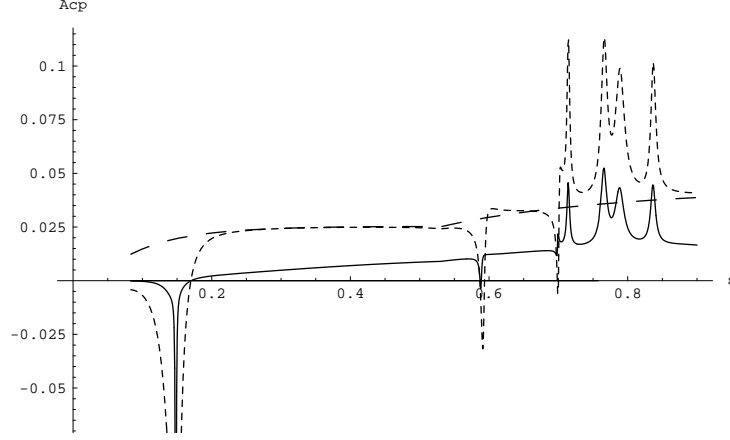


Figure 12: The same as Fig 11, but for fixed $\bar{\xi}_{N,bb}^D = 90 m_b$ value. .

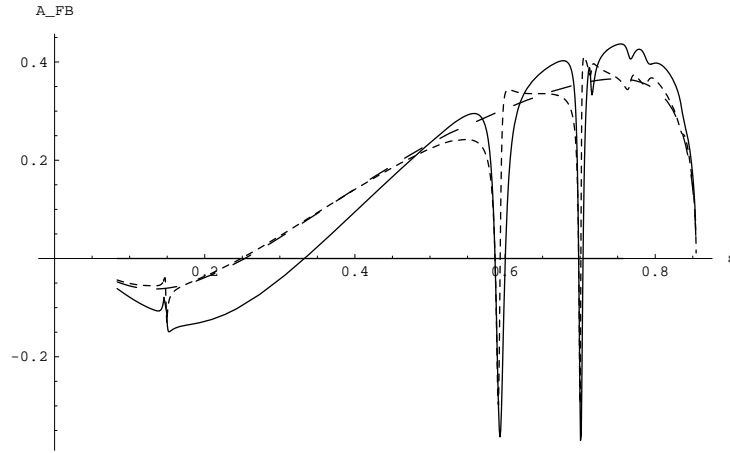


Figure 13: A_{FB} as a function of q^2 for fixed $\bar{\xi}_{N,bb}^D = 40 m_b$ in the region $|r_{tb}| \ll 1$, at the scale $\mu = m_b$ for the process $\bar{B} \rightarrow \rho e^+ e^-$. Here solid line and corresponds to the model III with LD effects, dashed line to the SM without LD effects and dotted dashed line to the SM with LD effects.

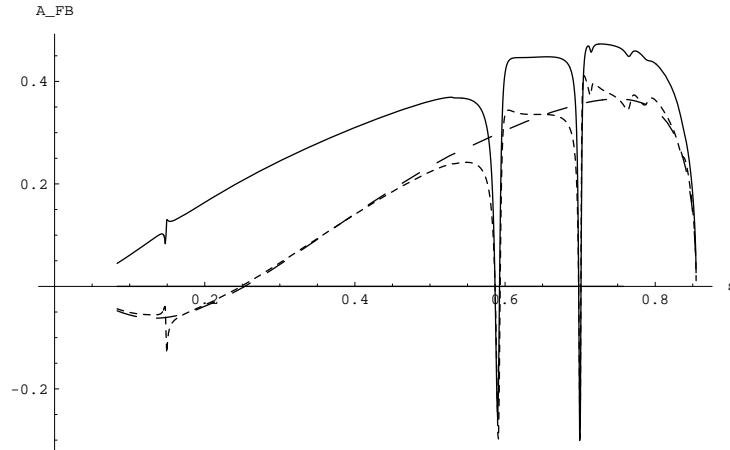


Figure 14: The same as Fig. 13, but at the region $r_{tb} \gg 1$.